Materials Science & Engineering A 733 (2018) 276–284

Contents lists available at ScienceDirect

Materials Science & Engineering A

journal homepage: www.elsevier.com/locate/msea

Grain boundary sliding and rotational mechanisms of intragranular deformation at different creep stages of high-purity aluminum polycrystals at various temperatures and stresses

V.E. Panin[a,b,*], N.S. Surikova[a], T.F. Elsukova[a], I.V. Vlasov[a], D.V. Borisyuk[a,b]

[a] Institute of Strength Physics and Materials Science SB RAS, Tomsk 634055, Russia
[b] National Research Tomsk Polytechnic University, Tomsk 634050, Russia

ARTICLE INFO

Keywords:
Creep
High-purity aluminum polycrystals
Grain boundary sliding
Plasticity methods
Grains and interfaces
Fracture

ABSTRACT

In the paper we show that grain boundary sliding dominates in the creep of A999 aluminum polycrystals and is accommodated by rotation modes of intragranular deformation. Accommodation mechanisms strongly depend on the applied stress σ and creep temperature T. At low σ and T, accommodation occurs by dislocation glide and mesoscale fragmentation. At high σ and T, there appears lattice curvature, which causes the development of shear bands, multiscale fragmentation, and formation of a quasi-neck with nanosized subgrains and plastic microrotations. Noncrystallographic shears in their subboundaries propagate in local lattice curvature zones under τ_{max} by the plastic distortion mechanism.

1. Introduction

It is known that grain boundary sliding plays an important role in creep deformation of polycrystals [1–10, etc.]. However, the question on primary mechanisms of deformation under creep is still discussed in the literature. Some authors [3–7] believe that grain boundary sliding results from the inhomogeneity of intragranular dislocation glide. Another opinion [8–11] is that grain boundary sliding is the leading process during creep, and intragranular deformation mechanisms accommodate rotation modes of grain boundary sliding. This opinion seems reliable since the polycrystal creeps at stresses below the yield point of the material. Moreover, the absence of translational invariance in grain boundaries ensures flows of point defects in them with the concentration much larger than the equilibrium concentration of vacancies in the grain crystal lattice [11–14].

Since grain boundary sliding is a translation-rotation mode of plastic deformation, intragranular slip must have a rotational component to obey the law of conservation of angular momentum. We previously showed [10] that at the tertiary stage of low-temperature creep of high-purity A999 aluminum polycrystals there occurs material separation in near-boundary zones, which sharply accelerates macroscopic deformation and ends in fracture of specimens loaded below their yield stress. This was explained by highly developed curvature of the crystal lattice in near-boundary zones of polycrystals under tertiary creep, which determines a high degree of self-consistency of grain boundary sliding and rotational mechanisms of intragranular deformation near grain boundaries [10]. This concept naturally requires that lattice curvature be measured in near-boundary zones of the polycrystal and this result be confirmed under various creep conditions. High curvature and misorientation of the crystal lattice in near-boundary zones of polycrystals of hexagonal close-packed metals due to grain boundary sliding were also discovered by Matsunaga et al. [4].

The aim of this paper is to investigate how temperature and applied stress affect the relation between grain boundary sliding and rotational mechanisms of intragranular deformation during creep of high-purity aluminum polycrystals. Mechanisms of low-temperature creep and diffusion creep are essentially different. However, their effect on the self-consistency of grain-boundary sliding and multiscale intragranular slip has not yet been investigated in the literature. In the mesomechanics of hierarchically organized systems, this issue is very relevant. Of special interest is the measurement of crystal lattice curvature to estimate its role in the self-consistency of grain-boundary sliding and rotational mechanisms of intragranular slip.

2. Materials and methods of investigation

The test material is high-purity polycrystalline aluminum (99.999 at %) that reveals highly pronounced normal grain boundary sliding and

* Corresponding author at: Institute of Strength Physics and Materials Science SB RAS, Tomsk 634055, Russia.
E-mail addresses: paninve@ispms.tsc.ru (V.E. Panin), surikova@ispms.tsc.ru (N.S. Surikova), elsukova@yandex.ru (T.F. Elsukova), good0@yandex.ru (I.V. Vlasov), dasha.94.5165@mail.ru (D.V. Borisyuk).

https://doi.org/10.1016/j.msea.2018.07.038
Received 27 March 2018; Received in revised form 4 July 2018; Accepted 11 July 2018
Available online 18 July 2018
0921-5093/

denuded zones of grain boundaries under low-temperature (T = 50 °C) creep at the pressure σ = 11–13 MPa [10]. The creep temperature is increased to 60 °C to study diffusion creep. The applied stress is varied within (11 − 18) MPa.

Flat dumbbell specimens with the gauge area 1.2 × 8 × 37 mm are produced from aluminum sheets with subsequent annealing during 0.5 h at 513 K. The size of Al polycrystalline grains is d = 400 µm. The specimen surface is prepared for structural studies by electrolytic polishing.

Creep tests are carried out in a specially made temperature controlled installation at T = 323 and 333 K under uniaxial loading. The specimen elongation is measured by dial indicators with the accuracy to ± 1 µm. The structure at different creep stages is viewed in optical (Axiovert 25CA), interference (New View 6200), transmission (JEOL 2100) and scanning (Quanta 200 3D) electron microscopes.

3. Results of investigation

3.1. Creep curves and mesoscopic mechanisms of deformation at T = 50 °C

Creep curves at $T = 50^oC$ and different stresses applied to specimens are shown in Fig. 1. Their stage character is well pronounced, although the tertiary stage is not achieved at σ = 11 MPa (but mechanisms of grain boundary sliding under steady-state creep were investigated in detail). At the primary creep stage, the degree of elongation of the specimens multiplies as the applied stress increases in the interval (11 − 18) MPa. The secondary and tertiary stages are shortened in this case. Upon fracturing after tertiary creep, the total plastic strain of the specimens is 32.4% at σ = 13 MPa and 40.5% at σ = 18 MPa. Grain boundary sliding and scale levels of mechanisms of intragranular accommodation deformation strongly depend on the stress applied to the specimens (Figs. 2–10).

Figs. 2 and 3 demonstrate the pattern of grain boundary sliding during creep at the applied stress σ = 11 and 13 MPa. Grain boundary sliding under low-stress creep has the following three features:

(i) Grain boundary sliding is normal to the specimen surface, thus resulting in high denuded grain boundaries; the maximum height of steps of grain boundary sliding at the stress σ = 11 MPa is ~ 18 µm (Fig. 2);
(ii) rotational deformation in the vicinity of sliding grain boundaries proves to be highly homogeneous and highly localized (Fig. 3). As was shown elsewhere [10], it occurs only by dislocation glide;
(iii) traces of plastic deformation are weakly pronounced on the main surface of grains along which grain boundary sliding develops.

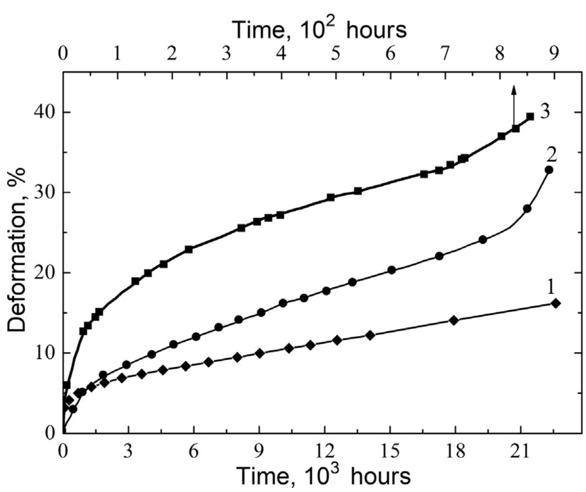

Fig. 1. Creep curves of high-purity A999 aluminum polycrystals at 323 K under different applied stresses: 11 (1), 13 (2) and 18 (3) MPa.

These results display that at low stresses translation-rotation modes of deformation are related mainly to grain boundaries and near-boundary zones of localized plastic flow.

With increasing stress to σ = 13 MPa, the maximum height of steps of grain boundary sliding is reduced to 7 µm (Fig. 3b) and accommodation slip bands develop on the surface of sliding grains (Fig. 3a). It is important to emphasize that the extrusion of grain vertexes during grain boundary sliding is always accompanied by their rotation. Thus, the rotation angle of the vertex of grain A is φ = 25° (Fig. 3b), and the rotation angle of grain B at the triple point of grains A-B-C is φ = 26° (Fig. 4). Separation of the oxide film from the surface of grain B in Fig. 4 makes possible detecting bands of single slip within the given grain during its extrusion and rotation. This points to layer-by-layer plastic deformation of grain B during grain boundary sliding along the denuded grain boundary.

The morphology of plastic deformation of the surface layer during grain boundary sliding under creep at the stress σ = 18 MPa changes sharply (Figs. 5 and 6). At grain boundary sliding the material is extruded when the tangential component of displacements increases sharply and normal displacements decrease (Fig. 6a). Thus, the height of vertical steps does not exceed 3 µm (Fig. 5b). The multiscale pattern of displacement of large fragments in the vicinity of the denuded grain boundary AB is represented in Fig. 6. The extrusion of grain C is seen to develop layer by layer, thus realizing rotation modes of deformation. Layers 1, 2, and 3 of grain C are displaced successively with respect to each other. Steps of viscous flow of the material ab, cd, ef arise between the layers. In each of the layers, extrusion also occurs by transverse displacement of individual blocks with the formation of transverse steps. According to Fig. 6b, the extrusion of the material in layer 1 of grain C during grain boundary sliding causes a material displacement to 6 µm. In this case, a fragment of grain C given in Fig. 6a realizes a complex rotational elastoplastic deformation by the mechanism of block shears. If zone B of grain C is displaced upwards (Fig. 6b) with a clockwise rotation of the vertex of the grain as a whole, then the block formation in layers 1, 2, and 3 occurs by their counterclockwise displacement. In other words, the self-consistency of grain boundary sliding and fragmentation of the extruded material satisfies the law of conservation of angular momentum.

Particular mention should be paid to the fragmentation and severe degradation of the structure of the outer layer of grain boundary sliding step AB (Fig. 6a). This material reveals layer-by-layer structural fragmentation in the grain boundary sliding direction indicated by the arrow. This is indicative of a high nonequilibrium of the material in the vicinity of sliding grain boundaries at the tertiary creep stage. As a consequence, plastic accommodation deformation in the near-boundary zone of adjacent grain D develops noncrystallographically. This should increase dramatically the creep rate and reduce the time to fracture by an order of magnitude.

Finally, the tertiary creep stage at the stress σ = 18 MPa culminates in the quasi-neck formation. Thinning of the specimen in this zone is accompanied by the development of the system of fine mesobands of localized plastic flow (Figs. 7 and 8). The height of steps formed during the propagation of such mesobands is about 2 µm (Fig. 7b). A step-like propagation of fine mesobands is detected at higher magnification (Fig. 8). As can be seen from Fig. 8, mesoband AB responsible for thinning of the specimen in the quasi-neck zone consists of fine transverse displacements with steps ~0.5 µm (Fig. 8b). This causes a submicron fragmentation of the material in the quasi-neck zone.

Since local grain boundary sliding results in local extrusion of the material, the law of conservation of the medium continuity explains the effect of intrusion of the appropriate material in the adjacent grain. This effect is represented in Fig. 9 and should be taken into account during multiscale grain boundary sliding.

We previously noted [10] that a high strain rate at the tertiary creep stage of A999 aluminum specimens at the stress σ = 13 MPa is associated with the separation of the highly nonequilibrium material in the